

Cite this: *Phys. Chem. Chem. Phys.*, 2011, **13**, 9824–9830

www.rsc.org/pccp

PAPER

Quantum fluctuations increase the self-diffusive motion of para-hydrogen in narrow carbon nanotubes†

Piotr Kowalczyk,^{*a} Piotr A. Gauden,^b Artur P. Terzyk^b and Sylwester Furmaniak^b

Received 21st January 2011, Accepted 24th March 2011

DOI: 10.1039/c1cp20184k

Quantum fluctuations significantly increase the self-diffusive motion of para-hydrogen adsorbed in narrow carbon nanotubes at 30 K comparing to its classical counterpart. Rigorous Feynman's path integral calculations reveal that self-diffusive motion of para-hydrogen in a narrow (6,6) carbon nanotube at 30 K and pore densities below ~ 29 mmol cm⁻³ is one order of magnitude faster than the classical counterpart. We find that the zero-point energy and tunneling significantly smoothed out the free energy landscape of para-hydrogen molecules adsorbed in a narrow (6,6) carbon nanotube. This promotes a delocalization of the confined para-hydrogen at 30 K (*i.e.*, population of unclassical paths due to quantum effects). Contrary the self-diffusive motion of classical para-hydrogen molecules in a narrow (6,6) carbon nanotube at 30 K is very slow. This is because classical para-hydrogen molecules undergo highly correlated movement when their collision diameter approached the carbon nanotube size (*i.e.*, anomalous diffusion in quasi-one dimensional pores). On the basis of current results we predict that narrow single-walled carbon nanotubes are promising nanoporous molecular sieves being able to separate para-hydrogen molecules from mixtures of classical particles at cryogenic temperatures.

Introduction

Confinement of classical and quantum particles at the nanoscale has attracted a lot of attention in recent years from a fundamental point of view as well as its relevance to nanotechnology, material science, biology, geology, astronomy, *etc.*^{1–10} The physical properties of confined particles and the diffusion rate in reduced dimensionality exhibit a number of peculiarities in comparison with the bulk phase.^{11–20} Among novel nanomaterials, single-walled carbon nanotubes (SWNTs) are excellent carbon nanomaterials providing a quasi-one dimensional nanoscale confinement.²¹ It is well-known that for classical particles anomalous single-file diffusion (SFD) occurs when the individual nanopores of the medium are so narrow that the particles are unable to pass each other.^{22–29} As a result, the sequence of particles remains the same over a long time. Because the movements of

individual particles are highly correlated, the mechanism of molecular diffusion in quasi-one dimensional nanopores is different from that observed for isotropic diffusion in the bulk system. Experimental and theoretical results collectively indicate that poorer mixing of adsorbed classical particles (*i.e.* traffic at the nanoscale) in narrow carbon nanotubes results in slow self-diffusive motion.^{22–29}

To the best of our knowledge the self-diffusive motion of light particles (*e.g.* ⁴He, para-H₂, ortho-D₂) adsorbed in quasi-one dimensional channels of carbon nanotubes at cryogenic temperatures has not been studied experimentally so far. It is not surprising since both quasielastic neutron scattering and pulsed-field gradient-nuclear magnetic resonance measurements of self-diffusion at cryogenic temperatures in narrow carbon nanotubes are very complicated. Individual carbon nanotubes of various sizes with metal contaminants and defects self-assemble into a stable bundle structure.^{21,30,31} This complex structure consists of different adsorption sites, including internal and interstitial channels, grooves, and rounded surface of the bundle. Thus, the measured overall self-diffusion constant of adsorbed particles does not correspond to this inside a defect-free carbon nanotube. Other experimental difficulties result from the instability of narrow carbon nanotubes characterized by a high graphene curvature as well as a poor experimental signal from light particles. Rigorous theoretical calculations and computer experiments offer an alternative tool for the investigation of the self-diffusive motion of light particles in narrow carbon nanotubes

^a Nanochemistry Research Institute, Department of Chemistry, Curtin University of Technology, P.O. Box U1987, Perth, 6845 Western Australia, Australia.

E-mail: Piotr.Kowalczyk@curtin.edu.au; Tel: +61 8 9266 7800

^b Department of Chemistry, Physicochemistry of Carbon Materials Research Group, N. Copernicus University, Gagarin St. 7, 87-100 Torun, Poland. E-mail: gaudi@uni.torun.pl, aterzyk@chem.uni.torun.pl, sf@chem.umk.pl

† Electronic supplementary information (ESI) available: Snapshots of p-H₂ and its classical counterpart adsorbed in studied carbon nanotubes (6_6mov1, 6_6mov2, class_mov1, class_mov2). Theory, methods, and simulation details with additional Fig. 1S–5S. It should be noted that all movies in the ESI were created using the VMD program.^{70,71}

at cryogenic temperatures. Due to low operating temperature and strong confinement, consideration of quantum effects (*i.e.*, zero-point energy and tunneling) in molecular simulations of light particles in narrow carbon nanotubes is absolutely crucial.^{32–40} Quantum dynamics at finite temperatures is a nontrivial problem of physics.⁴⁰ However, recent progress in this field allows reliable calculations of self-diffusion constants for distinguishable particles (*i.e.* Boltzmann particles). It has been shown by Rabani *et al.*,^{41,42} Hone *et al.*,^{43,44} and Miller III⁴⁵ that approximate methods of quantum dynamics generate similar values of self-diffusion constants for simple quantum fluids at finite temperatures.

Here for the first time, we demonstrate using rigorous theoretical calculations that a self-diffusive motion of parahydrogen (p-H₂) in narrow carbon nanotube channels at 30 K is significantly faster than its classical counterpart. When the effective diameter of the carbon nanotube approaches the effective size of the classical p-H₂ molecule (Lennard-Jones collision diameter ~ 2.589 Å) its self-diffusive motion is drastically reduced. Observed slow individual motion of p-H₂ classical molecules in narrow carbon nanotubes indicates the anomalous diffusion in quasi-one dimensional cylindrical carbon pores (see movies attached to ESI†). In contrast, computed self-diffusion constants for p-H₂ molecules in studied narrow carbon nanotubes are significantly greater because the quantum fluctuations impact their dynamics at 30 K.

We systematically investigated thermodynamic and dynamics properties of p-H₂ confined in selected carbon nanotubes at 30 K. For this purpose, we employed Feynman's path integral formulation of quantum mechanics at finite temperatures.³⁵ Following Ceperley,^{33,34} the degeneracy temperature can be estimated from the relation $T_D = \rho^{2/3} \hbar^2 / mk_B$, where ρ denotes density of the quantum fluid. At the highest studied density of the confined p-H₂ of 40 mmol cm⁻³, this temperature $T_D = 2$ K, and is far below the investigated temperature. We are thus confident that the Bose exchange effects do not influence our results within the numerical accuracy and thus can be neglected in our PIMC simulations. We computed the frequency-dependent diffusion constant, $D(\omega)$, for the bulk and adsorbed p-H₂ using analytic continuation of the imaginary-time correlation function.^{46–48} As previously discussed,⁴⁸ for the isotropic bulk p-H₂ we averaged the imaginary-time correlations over three dimensions (see comparison of experimental self-diffusion constants for liquid p-H₂ at 14 and 25 K with theoretical prediction presented in Fig. 2S–3S, ESI†). For p-H₂ molecules adsorbed in narrow carbon nanotubes, we averaged the imaginary-time correlations only in the axial direction (*i.e.* we report the self-diffusive motion of confined p-H₂ molecules along the nanotube). The self-diffusion constant corresponds to zero frequency absorption. For comparison we performed (classical) molecular dynamics (MD) of the p-H₂ classical counterpart for the same state points. To extract self-diffusion constants in the axial direction from our classical MD simulations we used standard Green–Kubo integration of the velocity autocorrelation function.^{49,50} To explain the results of real-time dynamics we computed the following properties: the free energy, kinetic and potential energy, high-temperature density matrix, and displacement correlation function in imaginary-time.

Theory, methods, and simulation details

The potential models, computational methodology, and their validation against known experimental data for the bulk parahydrogen at 14 and 25 K are documented in ESI.†

Results and discussion

We begin our discussion examining the effect of the carbon nanotube size on the self-diffusive motion of p-H₂ and its classical counterpart in the axial direction at 30 K (Fig. 1). Comparing to the bulk phase, confined p-H₂ molecules self-diffuse very similarly in all studied carbon nanotubes up to a pore density of ~ 24 mmol cm⁻³. Further increase in pore loading results in slower self-diffusive motion of adsorbed p-H₂ molecules comparing to the isotropic bulk because the strong confinement of p-H₂ molecules impact on their localization (see Fig. 2–6). As would be expected, self-diffusion constants for p-H₂ as well as its classical counterpart are different in wider ((10,10) and (12,12)) carbon nanotubes. At low densities (< 21 mmol cm⁻³), p-H₂ molecules self-diffuse more slowly than their classical counterparts. Interestingly, the

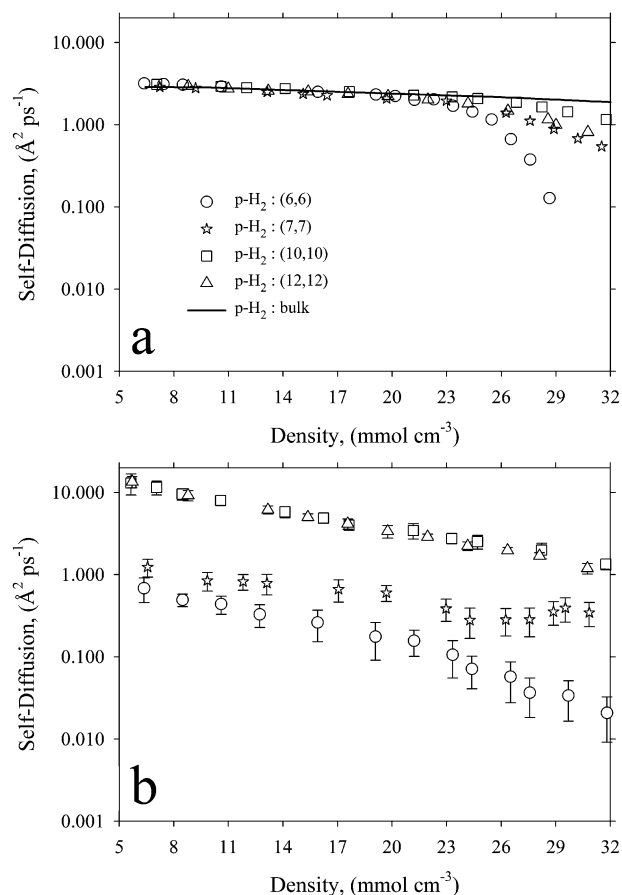


Fig. 1 Density dependence of PIMC (panel a) and classical (panel b) self-diffusion constants of p-H₂ adsorbed in studied carbon nanotubes at 30 K. PIMC and classical self-diffusion constants were computed from axial component of imaginary-time and velocity correlation functions, respectively. For comparison, the density dependence of PIMC self-diffusion constants computed for the isotropic bulk p-H₂ at 30 K is shown by a solid line.

lower is the adsorbed density, the larger are differences between self-diffusion constants for p-H₂ and its classical counterpart. This observation can be explained by a higher scattering probability of the delocalized p-H₂ in comparison to its classical counterpart at low pore densities. In contrast, for liquid-like densities of adsorbed fluids we observe very similar self-diffusive motion of studied particles up to 32 mmol cm⁻³. Fast quantum decoherence (*i.e.*, short time between intermolecular collisions) in dense adsorbed p-H₂ liquid can be responsible for this similarity. In narrow studied carbon nanotubes, we find different behaviour for self-diffusive motion of p-H₂ and its classical counterpart. As would be expected, the self-diffusion constants for the classical p-H₂ become progressively smaller with decreasing nanotube size.²⁹ Apart from this, we notice that the higher is the adsorbed density the slower the self-diffusive motion of classical p-H₂ molecules is. What is more interesting, for the narrowest (6,6) carbon nanotube, we predict that p-H₂ molecules self-diffuse one order of magnitude faster than their classical counterparts up to ~29 mmol cm⁻³. For higher pore densities, the computation of the self-diffusion constants from imaginary-time correlation functions is very difficult due to their small values and inherent numerical errors. The results depicted in Fig. 1, indicate a significant impact of quantum fluctuations at 30 K on the self-diffusive motion of the confined p-H₂ along nanotubes. To gain a better understanding of this spectacular self-diffusive motion of p-H₂ in narrow (6,6) and (7,7) carbon nanotubes, we computed and examined a number of other properties.

First, we consider the plots of frequency–diffusion constants for the bulk and confined p-H₂ at 30 K presented in Fig. 2. Regardless the size of carbon nanotubes and pore loading, we find that quasi-one dimensional confinement significantly influences the p-H₂ power spectrum at 30 K. In comparison to the bulk p-H₂, we notice a blueshift in the position of the maximum of $D(\omega)$, an increase in the phonon density of states at intermediate and high frequencies, and a decrease in the phonon density of states at low frequencies. However, for all studied adsorption systems, we do not observe the energy gap between the ground-state and lowest-energy excited states. For low densities of the confined p-H₂ we observe a sharp peak on $D(\omega)$. This peak is gradually smoothed out with pore loading. A drop in the self-diffusion constant (*i.e.*, the drop in zero frequency absorption) is matched by the appearance of a peak at finite frequencies, and the position of this peak increases as the self-diffusion constant decreases. As shown by Chandler *et al.*^{51–53} and others,^{45,54} all counted variations in the $D(\omega)$ spectrum with density result from stronger localization of adsorbed p-H₂ molecules in comparison to the bulk ones. Thus to a first approximation, adsorbed p-H₂ fluids look at higher effective densities like bulk ones (*i.e.* nanoconfinement shifts the phase diagram of the adsorbed p-H₂).

Fig. 3 shows density variation of the PIMC kinetic and potential energy computed for the bulk and confined p-H₂ at 30 K. Due to strong localization of p-H₂ molecules in the solid–fluid potential well, the exact value of the kinetic energy of adsorbed molecules exceeds this corresponding to the bulk phase. Quantum fluctuations in momentum space at zero coverage are reflected in the excess value of kinetic energy

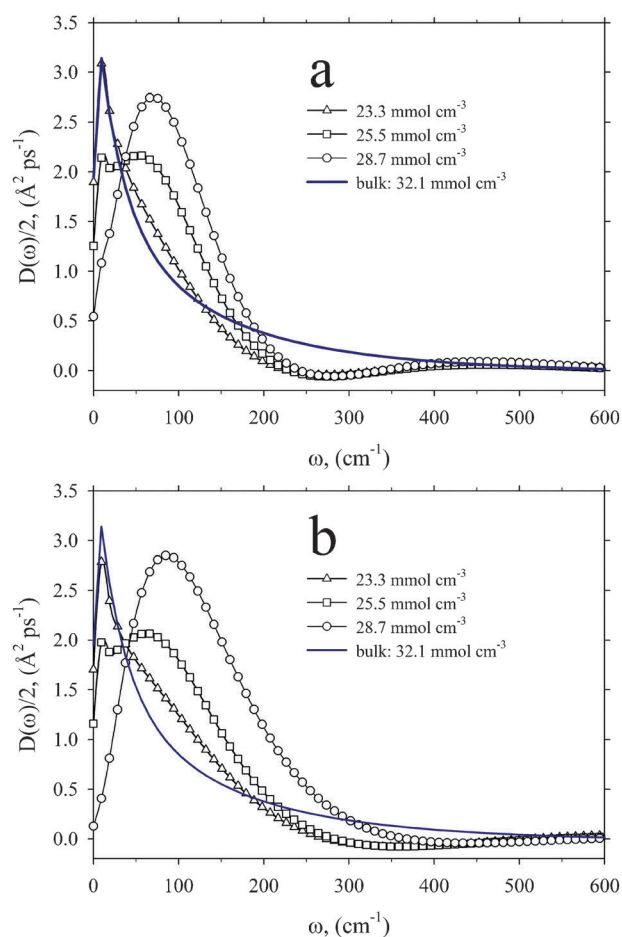


Fig. 2 The frequency-dependent diffusion constant computed for selected densities of p-H₂ adsorbed in (7,7) (upper panel) and (6,6) (bottom panel) carbon nanotubes at 30 K. Presented $D(\omega)$ power spectra were computed from the axial component of imaginary-time correlation functions. For comparison, the $D(\omega)$ power spectrum computed for the isotropic bulk p-H₂ at 30 K is shown by solid line.

strongly depending on the nanotube size (more precisely, the shape and depth of the solid–fluid potential). As would be expected, the higher is the pore loading the larger the kinetic energy of adsorbed and compressed p-H₂ fluid is. This is caused by additional fluid–fluid interactions further increasing localization of confined p-H₂ molecules. The most spectacular variation in PIMC kinetic energy is observed for the narrowest (6,6) carbon nanotube, as is displayed in Fig. 3. High localization of adsorbed p-H₂ molecules due to steep solid–fluid potential and adsorbed neighbours results in a rapid increase in kinetic energy with pore densities above ~25 mmol cm⁻³. This also indicates that the variation of the many-body potential energy surface with pore loading is the highest for the narrowest (6,6) carbon nanotube. Using simplified classical reasoning, we can imagine p-H₂ molecules adsorbed and compressed inside the (6,6) carbon nanotube as their very hot classical counterparts.^{55–57} It is worth to point out that a rapid rise in the kinetic energy of the confined p-H₂ is fully consistent with the fundamental Heisenberg’s uncertainty principle. Quantum fluctuations in steep-solid fluid potential (*i.e.*, strong localization in the positional space) are responsible for high momentum of

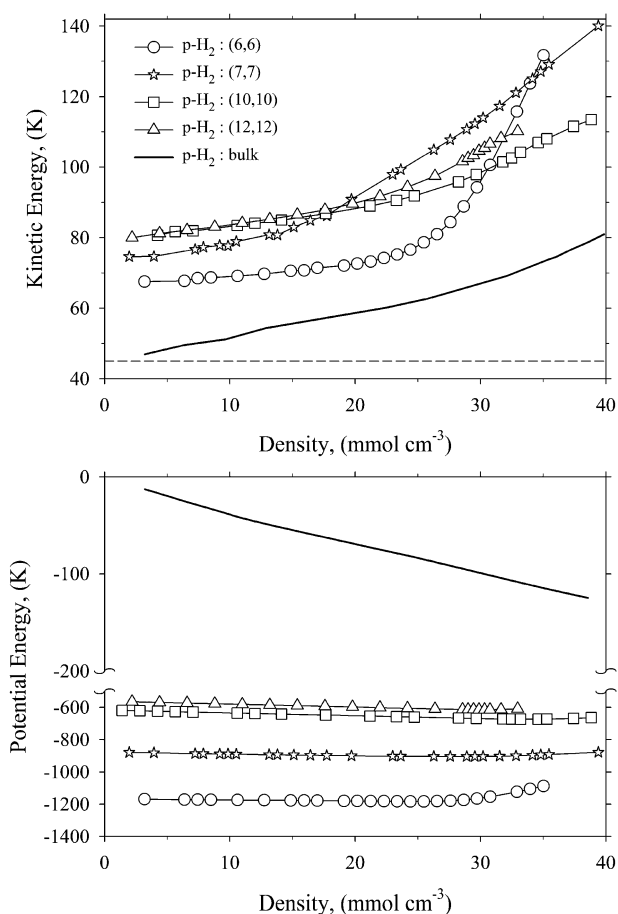


Fig. 3 Density dependence of PIMC kinetic and potential energy of p-H₂ adsorbed in studied carbon nanotubes at 30 K. For comparison, density dependence of PIMC kinetic and potential energy for the bulk p-H₂ at 30 K is shown by solid lines. The classical kinetic energy, $3/2k_B T = 45$ K, is displayed by a dashed line on the upper panel.

adsorbed p-H₂ molecules. In contrast, PIMC potential energy slightly depends on pore loading, as is presented in Fig. 3. The value of the potential energy is much lower in comparison to the bulk phase and strongly correlates with the nanotube size. In all studied carbon nanotubes, the potential energy of the adsorbed p-H₂ at 30 K is dominated by a high solid–fluid interaction potential generated from interactions with nanotube walls.

Fig. 4 depicts the comparison of PIMC and classical free energy values computed for selected p-H₂ pore loading at 30 K. Regardless the size of studied carbon nanotube, we find that quantum fluctuations reduce the classical free energy barrier at the pore centre. The flatter free energy landscape in narrow nanotubes destabilizes the localization of p-H₂ molecules as opposed to their classical counterparts. For all studied pore loading classical p-H₂ molecules are trapped in the solid–fluid potential minima close to the pore wall. Thus, the penetration of the (6,6) nanotube space near the pore centre by classical p-H₂ molecules is an infrequent event, as is shown in Fig. 5. In contrast, the excess of kinetic energy due to quantum fluctuations increases the number of unclassical paths (*i.e.*, classically forbidden trajectories) promoting the self-diffusive motion of p-H₂ molecules towards the (6,6) nanotube centre. In wider nanotubes, *e.g.* (10,10) and (12,12),

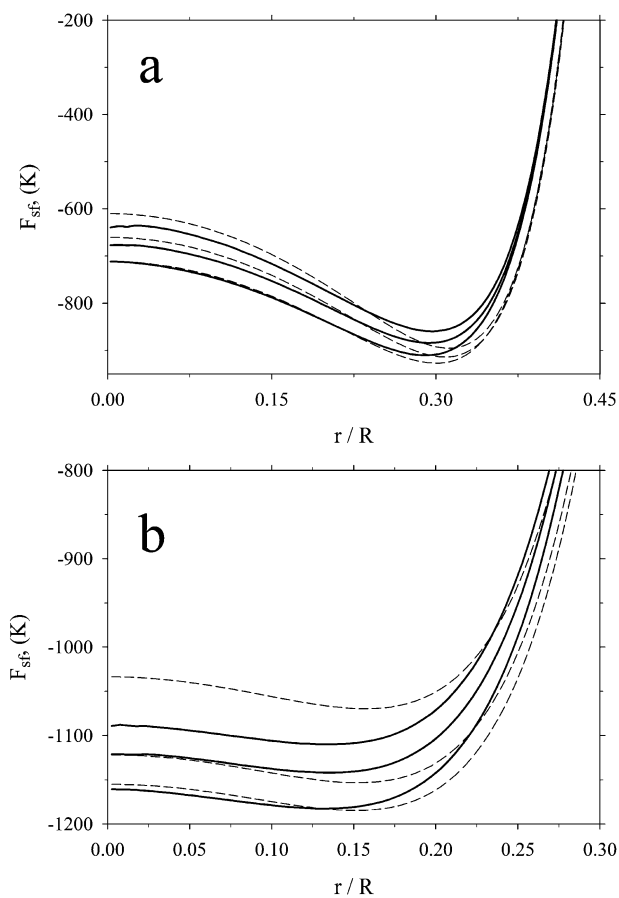


Fig. 4 Density dependence of PIMC (solid lines) and classical (MC—dashed lines) free energy of p-H₂ adsorbed in (7,7) (panel a) and (6,6) (panel b) carbon nanotubes at 30 K. Studied densities are: 1, 20, and 26 mmol cm⁻³.

the free energy barrier at the pore centre is very high (see Table 1, and Fig. 1S, ESI†). Quantum fluctuations of p-H₂ at 30 K are unable to smooth out the free energy landscape significantly. As a result, both p-H₂ molecules and their classical counterparts are localized close to the pore wall (see Fig. 5S, ESI†). That is why their self-diffusive motion is very similar in liquid-like adsorbed phases.

To gain insight into delocalization of adsorbed p-H₂ molecules in narrow nanotubes we compared PIMC and classical high-temperature density matrix for selected pore loading (see Fig. 5). First, we notice that MD results are in full agreement with the PIMC calculations in the classical limit (*i.e.*, PIMC with one bead per cyclic polymer chain). We find a significant number of unclassical paths for p-H₂ adsorbed in narrow (6,6) and (7,7) nanotubes. Observed growing delocalization of p-H₂ in comparison to its classical counterpart is fully consistent with the calculations of the free energy profiles. Adsorbed p-H₂ molecules are able to penetrate the classically forbidden regions of the narrow (6,6) nanotube space near the pore centre. We believe that this is reflected in higher values of PIMC self-diffusion constants of adsorbed p-H₂ molecules in comparison to their classical counterparts. Additionally one can see that the number of unclassical paths is reduced with pore loading. As pore density increases the

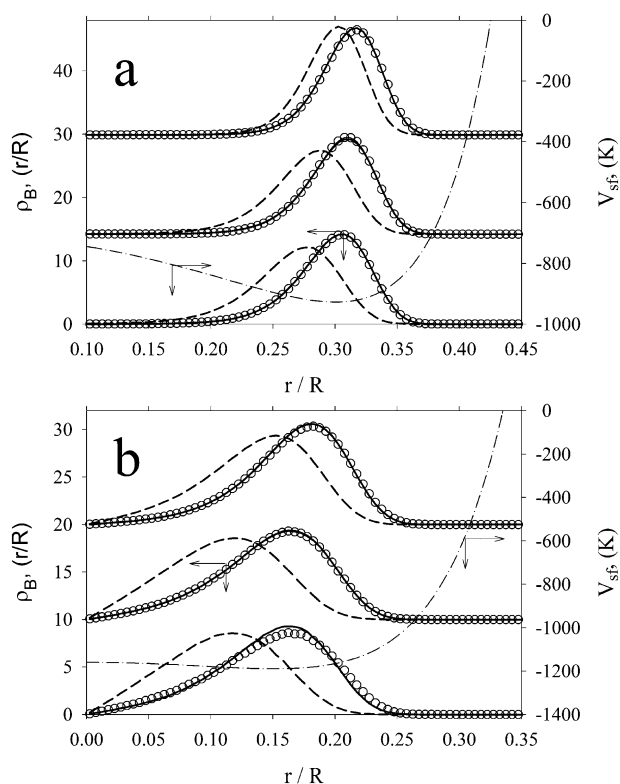


Fig. 5 Density dependence of PIMC (dashed lines) and classical (solid lines) and MD (open circles) high-temperature density matrix of p-H₂ adsorbed in (7,7) (panel a) and (6,6) (panel b) carbon nanotubes at 30 K. Studied densities are: 7 (bottom panel), 20 (middle panel), and 32 mmol cm⁻³ (upper panel). The solid–fluid interaction potential is displayed by dash-dotted lines.

Table 1 Free energy barriers, ΔF_{sf} , and kinetic energies of the adsorbed p-H₂, E_{kin} , at infinite dilution computed from PIMC simulations. Reduced effective nanotube diameter, D_e , is defined as D/σ_{ff} , where D denotes the space in carbon nanotubes where the solid–fluid potential is attractive, and $\sigma_{\text{ff}} = 2.598 \text{ \AA}$ denotes the (12,6) Lennard-Jones collision diameter for p-H₂

Parameter	Nanotube			
	(6,6)	(7,7)	(10,10)	(12,12)
$\Delta F_{\text{sf}}/\text{K}$	29.3	215.5	491.1	528.0
E_{kin}/K	67.5	74.6	79.6	80.0
D_e	1.05	1.54	3.08	4.14

path's centroid is more localized close to the pore wall (see Fig. 5). As is theoretically justified,⁵³ a growing localization of p-H₂ molecules with pore loading slows down their self-diffusion rate. Thus, for investigated operating conditions we predict that the self-diffusive motion of p-H₂ fluid confined in all studied carbon nanotubes at zero converge is always greater in comparison to finite densities.

As shown by Chandler *et al.*,^{51,58} Berne *et al.*,^{59,60} Miller III *et al.*,^{45,61} and others,^{38,62} the mean square displacement correlation function, $R^2(\tau)$, provides a quantitative measure of the path's structure. The loss of time dependence in $R^2(\tau)$ indicates the localized state of the quantum particle (*i.e.*, collapse of Feynman's polymer chain). In the localized state a self-diffusive motion of quantum particle slows down

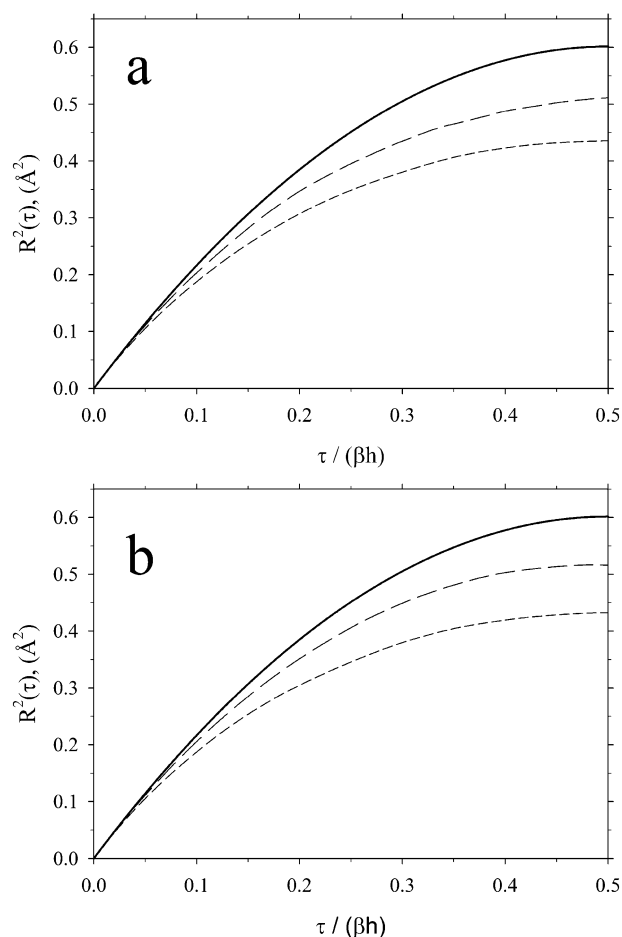


Fig. 6 PIMC imaginary-time correlation functions computed for p-H₂ adsorbed in (7,7) (panel a) and (6,6) (panel b) carbon nanotubes at 30 K. Studied densities for a (7,7) carbon nanotube are: 7 (long dashed lines), and 26 mmol cm⁻³ (short dashed lines). Studied densities for a (6,6) carbon nanotube are: 11 (long dashed lines), and 32 mmol cm⁻³ (short dashed lines). For comparison, the imaginary-time correlation functions computed for the free p-H₂ molecule are displayed by solid lines.

because of the limited accessibility to the extended states configurations.^{51,59} The increased localization of p-H₂ molecules adsorbed in narrow nanotubes with increasing pore density is clearly seen in Fig. 6. Interestingly for both narrow ((6,6) and (7,7)) nanotubes the extend of polymer shrinking with pore density is similar. The spatial extend of the free p-H₂ at 30 K, $R^2(\beta\hbar/2)$, is 0.6 \AA^2 . Strong confinement of the p-H₂ molecule in narrow nanotubes reduced its spatial extent down to $\sim 0.4 \text{ \AA}^2$. However, the key observation is that the confined polymer chains do not collapse into ground state (see the lack of plateau in Fig. 6). This observation supports similar self-diffusive motion of adsorbed p-H₂ molecules in both carbon nanotubes at 30 K over the wide range of pore densities, as is shown in Fig. 1.

The main motivation for this work comes from the lack of fundamental understanding of quantum dynamics in narrow carbon nanotubes at finite temperatures. Our results are in accordance with path integral calculations published by different authors. As others,^{63–69} we find a softening of the

classical free energy barrier by quantum fluctuations at finite temperatures. The zero-point motion and tunneling increases delocalization of quantum particles in comparison to classical ones. This affects not only thermodynamic properties of confined p-H₂ molecules, but also significantly impacts their self-diffusive motion at cryogenic temperatures. Obviously, self-diffusive motion of p-H₂ in host material at low temperatures can be affected by point defects, metal impurities, functional groups, *etc.*, because random disorder always promotes localization of quantum particles.⁵¹ Nevertheless, for homogenous narrow carbon nanotubes (such as (6,6) single-walled carbon nanotube) one would expect rapid decreasing of self-diffusive motion for all classical particles at cryogenic operating conditions. For the same operating conditions, the self-diffusion rate of p-H₂ in narrow carbon nanotubes is expected to be much higher because of the quantum nature. Why narrow (6,6) and (7,7) carbon nanotubes are so special? The answer to this question is straightforward. The free energy barrier inside narrow carbon nanotubes is much smaller in comparison to wider ones. Thus, the free energy landscape is significantly smoothed out by quantum fluctuations at 30 K. Taking into account our theoretical results we believe that homogenous narrow carbon nanotubes are promising nanomaterials for construction of novel devices (*i.e.*, nanofilters being able to separate p-H₂ molecules from mixtures of classical particles at cryogenic operating conditions). This is justified by the fact that all classical molecules of technological interests (*e.g.* argon, xenon, methane, carbon dioxide, sulfur dioxide, carbon monoxide, and others) are characterized by a higher effective size than the studied p-H₂ classical counterpart. Lowering operating temperature would result in better performance of nanofilters due to increasing quantum fluctuations. Although our theoretical calculations shed new light on the problem of quantum dynamics of light particles in strong nanoconfinement at cryogenic temperatures, more theoretical and experimental works are needed to fully explore the potential of fascinating novel nanomaterials in separation science and technology.

Acknowledgements

Piotr Kowalczyk gratefully acknowledges Prof. Eran Rabani (Tel Aviv University, Israel) and Dr Manolo Per (RMIT University, Australia) for fruitful discussions on the content of the current paper. P.K. acknowledges partial support by the Office of Research & Development, Curtin University of Technology, Grant CRF10084. Piotr Gauden and Artur Terzyk acknowledge the use of the computer cluster at the Poznan Supercomputing and Networking Centre as well as the Information and Communication Technology Centre of Nicolaus Copernicus University (Torun, Poland). Sylwester Furmaniak gratefully acknowledges financial support from the Foundation for Polish Science.

References

- Y. Gogotsi, R. K. Dash, G. Yushin, T. Yildirim, G. Laudisio and J. E. Fischer, *J. Am. Chem. Soc.*, 2005, **127**, 16006–16007.
- H. Tanaka, H. Kanoh, M. Yudasaka, S. Iijima and K. Kaneko, *J. Am. Chem. Soc.*, 2005, **127**, 7511–7516.
- P. Kowalczyk, R. Holyst, M. Terrones and H. Terrones, *Phys. Chem. Chem. Phys.*, 2007, **9**, 1786–1792.
- R. Banerjee, A. Phan, B. Wang, C. Knobler, H. Furukawa, M. O’Keeffe and O. M. Yaghi, *Science*, 2008, **319**, 939–943.
- B. Liu, X. Li, B. Li, B. Xu and Y. Zhao, *Nano Lett.*, 2009, **9**, 1386–1394.
- P. Kowalczyk, A. Ciach and A. V. Neimark, *Langmuir*, 2008, **24**, 6603–6608.
- M. Endo, H. Muramatsu, T. Hayashi, Y. A. Kim, M. Terrones and M. S. Dresselhaus, *Nature*, 2005, **433**, 476.
- Y. Tao, H. Muramatsu, M. Endo and K. Kaneko, *J. Am. Chem. Soc.*, 2010, **132**, 1214–1215.
- A. Witze, *Nature*, 2008, **456**, 290.
- S. Keskin, J. Liu, R. B. Rankin, J. K. Johnson and D. S. Sholl, *Ind. Eng. Chem. Res.*, 2009, **48**, 2355–2371.
- L. D. Gelb, K. E. Gubbins, R. Radhakrishnan and M. Sliwinski-Bartkowiak, *Rep. Prog. Phys.*, 1999, **62**, 1573–1659.
- C. Rasmussen, A. Vishnyakov, M. Thommes, B. Smarsly, F. Kleitz and A. V. Neimark, *Langmuir*, 2010, **26**, 10147–10157.
- P. Kowalczyk, H. Tanaka, R. Holyst, K. Kaneko, T. Ohmori and J. Miyamoto, *J. Phys. Chem. B*, 2005, **109**, 17174–17183.
- A. Kondo, H. Noguchi, S. Ohnishi, H. Kajiro, A. Tohdoh, Y. Hattori, W.-Ch. Xu, H. Tanaka, H. Kanoh and K. Kaneko, *Nano Lett.*, 2006, **6**, 2581–2584.
- B. Smarsly, M. Thommes, P. I. Ravikovitch and A. V. Neimark, *Langmuir*, 2006, **22**, 756–764.
- F. R. Hung, B. Coasne, E. E. Santiso, K. E. Gubbins, F. R. Siperstein and M. Sliwinski-Bartkowiak, *J. Chem. Phys.*, 2005, **122**, 144706–144714.
- A. Kondo, H. Noguchi, L. Carlucci, D. M. Proserpio, G. Ciani, H. Kajiro, T. Ohba, H. Kanoh and K. Kaneko, *J. Am. Chem. Soc.*, 2007, **127**, 12362–12363.
- J. Hoffmann and P. Nielaba, *Phys. Rev. E: Stat. Phys., Plasmas, Fluids, Relat. Interdiscip. Top.*, 2003, **67**, 036115.
- P. Kowalczyk, L. Solarz, D. D. Do, A. Samborski and J. M. MacElroy, *Langmuir*, 2006, **22**, 9035–9040.
- D. Britt, H. Furukawa, B. Wang, T. G. Glover and O. M. Yaghi, *Proc. Natl. Acad. Sci. U. S. A.*, 2009, **106**, 20637–20640.
- S. Iijima, *Nature*, 1991, **354**, 56–58.
- J. Kärger and D. M. Ruthven, *Diffusion in zeolites and other microporous solids*, John Wiley & Sons, New York, 1992.
- A. Das, S. Jayanthi, H. Deepak, K. V. Ramanathan, A. Kumar, C. Dasgupta and A. K. Sood, *ACS Nano*, 2010, **4**, 1687–1695.
- K. Hahn, J. Kärger and V. Kukla, *Phys. Rev. Lett.*, 1996, **76**, 2762–2765.
- Q.-H. Wei, C. Bechinger and P. Leiderer, *Science*, 2000, **287**, 625–627.
- V. Kukla, J. Kornatowski, D. Demuth, I. Girnus, H. Pfeifer, L. V. C. Rees, S. Schunk, K. K. Unger and J. Kärger, *Science*, 1996, **272**, 702–704.
- D. Keffer, A. V. McCormick and H. T. Davis, *Mol. Phys.*, 1996, **87**, 367–387.
- D. S. Sholl and K. A. Fichthorn, *Phys. Rev. Lett.*, 1997, **79**, 3569–3572.
- Q. Chen, J. D. Moore, Y.-Ch. Liu, T. J. Roussel, Q. Wang, T. Wu and K. E. Gubbins, *J. Chem. Phys.*, 2010, **133**, 094501.
- Carbon Materials—Theory and Practice*, eds. A. P. Terzyk, P. A. Gauden and P. Kowalczyk, Research Signpost, Kerala, 2008.
- S. Iijima, M. Yudasaka, R. Yamada, S. Bandow, K. Suenaga and F. Kokai, *Chem. Phys. Lett.*, 1999, **309**, 165–170.
- D. Chandler, In *Theory of Quantum Processes in Liquids*, eds. J. P. Hansen, D. Levesque and J. Zinn-Justin, Elsevier, Amsterdam, The Netherlands, 1991.
- D. M. Ceperley, *Rev. Mod. Phys.*, 1995, **67**, 279–355.
- D. M. Ceperley, *Rev. Mod. Phys.*, 1999, **71**, S438–443.
- R. P. Feynman and A. Hibbs, *Quantum Mechanics and Path Integrals*, McGraw-Hill, New York, 1965.
- S. R. Challa, D. Sholl and J. K. Johnson, *Phys. Rev. B: Condens. Matter*, 2001, **63**, 245419.
- P. Kowalczyk, P. A. Gauden and A. P. Terzyk, *J. Phys. Chem. B*, 2008, **112**, 8275–8284.
- M. E. Tuckerman, *Statistical Mechanics: Theory and Molecular Simulation*, Oxford University Press, Oxford, 2010.
- D. Chandler and P. G. Wolynes, *J. Chem. Phys.*, 1981, **74**, 4078–4095.

- 40 M. E. Tuckerman, G. J. Martyna, M. L. Klein and B. J. Berne, *J. Chem. Phys.*, 1993, **99**, 2796–2808.
- 41 E. Rabani, G. Krilov, D. R. Reichman and B. J. Berne, *J. Chem. Phys.*, 2005, **123**, 184506.
- 42 O. Kletenik-Edelman, E. Rabani and D. R. Reichman, *Chem. Phys.*, 2010, **370**, 132–136.
- 43 T. D. Hone, P. J. Rossky and G. A. Voth, *J. Chem. Phys.*, 2006, **124**, 154103.
- 44 T. D. Hone, J. A. Poulsen, P. J. Rossky and D. E. Manolopoulos, *J. Phys. Chem. B*, 2008, **112**, 294–300.
- 45 T. F. Miller III, *J. Chem. Phys.*, 2008, **129**, 194502.
- 46 E. Rabani, D. R. Reichman, G. Krilov and B. J. Berne, *Proc. Natl. Acad. Sci. U. S. A.*, 2002, **99**, 1129–1133.
- 47 S. Habershon, B. J. Braams and D. E. Manolopoulos, *J. Chem. Phys.*, 2007, **127**, 174108.
- 48 P. Kowalczyk, P. A. Gauden, A. P. Terzyk and S. Furmaniak, *J. Chem. Theory Comput.*, 2009, **5**, 1990–1996.
- 49 M. P. Allen and D. J. Tildesley, *Computer Simulation of Liquids*, Clarendon, Oxford, 1987.
- 50 D. Frenkel and B. Smit, *Understanding Molecular Simulation From Algorithms To Applications*, Academic Press, London, 1996.
- 51 D. Chandler and K. Leung, *Annu. Rev. Phys. Chem.*, 1994, **45**, 557–591.
- 52 A. L. Nichols, D. Chandler, Y. Singh and D. M. Richardson, *J. Chem. Phys.*, 1984, **81**, 5109–5116.
- 53 A. L. Nichols and D. Chandler, *J. Chem. Phys.*, 1987, **87**, 6671–6681.
- 54 T. D. Hone and G. A. Voth, *J. Chem. Phys.*, 2004, **121**, 6412–6422.
- 55 C. M. Ceperley and E. L. Pollock, *Can. J. Phys.*, 1987, **65**, 1416.
- 56 P. Kowalczyk, L. Brualla, P. A. Gauden and A. P. Terzyk, *Phys. Chem. Chem. Phys.*, 2009, **11**, 9182–9187.
- 57 P. Kowalczyk, P. A. Gauden and A. P. Terzyk, *J. Phys. Chem. B*, 2010, **114**, 5047–5052.
- 58 M. Sprik, M. L. Klein and D. Chandler, *Phys. Rev. B: Condens. Matter*, 1985, **31**, 4234–4244.
- 59 B. J. Berne, *J. Stat. Phys.*, 1986, **43**, 911–929.
- 60 D. F. Coker, B. J. Berne and D. Thirumalai, *J. Chem. Phys.*, 1987, **86**, 5689–5702.
- 61 A. R. Menzeleev and T. F. Miller III, *J. Chem. Phys.*, 2010, **132**, 034106.
- 62 A. Pérez, M. E. Tuckerman and M. H. Müser, *J. Chem. Phys.*, 2009, **130**, 184105.
- 63 M. E. Tuckerman, D. Marx, M. L. Klein and M. Parrinello, *Science*, 1997, **275**, 817.
- 64 X.-Z. Li, M. I. J. Probert, A. Alavi and A. Michaelides, *Phys. Rev. Lett.*, 2010, **104**, 066102.
- 65 K. Kinugawa, P. B. Moore and M. L. Klein, *J. Chem. Phys.*, 1998, **109**, 610–617.
- 66 Ch. Chakravarty, *J. Chem. Phys.*, 2002, **116**, 8938–8947.
- 67 M. E. Tuckerman, D. Marx and M. Parrinello, *Nature*, 2002, **417**, 925–929.
- 68 H. S. Mei, M. E. Tuckerman, D. E. Sagnella and M. L. Klein, *J. Phys. Chem. B*, 1998, **102**, 10446–10458.
- 69 A. Witt, S. D. Ivanov, M. Shiga, H. Forbert and D. Marx, *J. Chem. Phys.*, 2009, **130**, 194510.
- 70 W. Humphrey, A. Dalke and K. Schulten, *J. Mol. Graphics*, 1996, **14**, 33–38.
- 71 Visual Molecular Dynamics. <http://www.ks.uiuc.edu/Research/vmd/>.